Nanoscale

PAPER

View Article Online
View Journal | View Issue

Cite this: *Nanoscale*, 2014, **6**, 13550

A microscale thermophoretic turbine driven by external diffusive heat flux†

Mingcheng Yang,*[a] Rui Liu,[a] Marisol Ripoll[b] and Ke Chen*[a]

Received 15th July 2014,
Accepted 8th September 2014

DOI: 10.1039/c4nr03990d

www.rsc.org/nanoscale

We propose a theoretical prototype of a micro-scale turbine externally driven by diffusive heat flux without the need for macroscopic particle flux, which is in sharp contrast to conventional turbines. The prototypes are described analytically and validated by computer simulations. Our results indicate that a micro-scale turbine composed of anisotropic blades can rotate unidirectionally in an external temperature gradient due to the anisotropic thermophoresis effect. The rotational direction and speed depend on the temperature gradient, the geometry and the thermophoretic properties of the turbine. The proposed thermophoretic turbines can be experimentally realized and implemented on micro-devices such as computer-chips to recover waste heat or to facilitate cooling.

Introduction

In the last century, the population growth and the rapid increase of technological demand has translated into an exponential rise of the world energy consumption. In most industrial and everyday processes, enormous amounts of energy are being wasted through heat dissipation. Waste heat recovery is thus critical from an economical and an environmental viewpoint. Two important devices for recycling waste heat are traditional heat engines like the Stirling engine and thermoelectric generators. Conventional heat engines operate efficiently through the expansion and compression of working fluids, but are quite difficult to scale down to microscales,[1] where thermal gradients are ubiquitous. Although small in terms of power, the recovery of waste heat from microchips and other electronic components represents a significant challenge. Thermoelectric generators, which convert heat flux into electricity by the Seebeck effect of solid-state materials, are robust and easy to miniaturize.[2,3] However, the applications of these devices have been largely limited by their low operational efficiency and high costs. Besides the search for better thermoelectric materials, finding out novel strategies to recover such waste heat is of great practical and fundamental importance and could have an enormous economic impact.

In this work, we propose theoretically a microscale turbine that can rotate in an external temperature gradient due to anisotropic thermophoresis. The character of external-temperature-gradient-driving allows the micro-turbine to harvest mechanical work directly from waste heat. This is in contrast to other existing thermophoretic rotors[4,5] which are self-propelled by local temperature gradients. Moreover, the proposed micro-turbine is driven by purely diffusive heat flux, and it is fundamentally different from conventional turbines that are driven by convective particle fluxes. This conceptually new thermophoretic turbine constitutes an important complement to existing turbines. Our work thus opens up new possibilities for recycling waste heat and designing turbines, and also provides new insights into thermophoresis of anisotropic objects.

Theory: anisotropic thermophoresis and thermophoretic turbine

In solutions with thermal inhomogeneities, suspended particles exhibit directional drift along or against the temperature gradient, a phenomenon known as thermophoresis, thermodiffusion or the Soret effect.[6–9] Practical applications of this effect are numerous, including manipulation of macromolecules in solution,[10–12] analysis of protein interactions in biological liquids[13] or the design of self-propelled micro-objects.[4,5,14] The driving force for thermophoresis, namely the thermophoretic force, arises from the interactions between particles and the surrounding inhomogeneous fluid environment induced by the temperature gradient,[15–18] and is related to the temperature gradient ∇T by

$$\boldsymbol{f} = -\alpha_{\mathrm{T}} k_{\mathrm{B}} \nabla T. \quad (1)$$

[a]*Beijing National Laboratory for Condensed Matter Physics and Key Laboratory of Soft Matter Physics, Institute of Physics, Chinese Academy of Sciences, Beijing 100190, China. E-mail: mcyang@iphy.ac.cn, kechen@iphy.ac.cn*
[b]*Theoretical Soft-Matter and Biophysics, Institute of Complex Systems, Forschungszentrum Jülich, 52425 Jülich, Germany*

†Electronic supplementary information (ESI) available. See DOI: 10.1039/c4nr03990d

Here, k_B is the Boltzmann constant and the dimensionless coefficient α_T is known as the thermodiffusion factor. This coefficient is determined by the specific properties of the particles and the solvent, and it is very sensitive to a large number of factors such as the average temperature or density. By convention, $\alpha_T > 0$ and $\alpha_T < 0$ respectively correspond to thermophobic and thermophilic behaviors.

Thermophoresis of isotropic objects is characterized by a unique value of the thermodiffusion factor (scalar), such that the thermophoretic force always occurs in the direction of the temperature gradient. This is however not the general case for anisotropic objects, where multiple thermodiffusion factors (tensor) are needed. As a consequence, the thermophoretic force applied on an anisotropic particle can eventually have a non-vanishing component perpendicular to the temperature gradient. To demonstrate this, we first consider a simple ellipsoidal particle in a non-isothermal solution, as shown in Fig. 1a. The thermophoretic anisotropy of the particle is characterized by thermodiffusion factors along the short and long axes, $\alpha_{T,s}$ and $\alpha_{T,l}$, and then the thermophoretic forces along these two axes can be separately calculated as

$$\boldsymbol{f}_s = -\alpha_{T,s} k_B \sin\theta |\nabla T| \boldsymbol{n}_s \quad (2)$$

and

$$\boldsymbol{f}_l = -\alpha_{T,l} k_B \cos\theta |\nabla T| \boldsymbol{n}_l. \quad (3)$$

Here, θ is the included angle between the particle long axis and ∇T, and $\boldsymbol{n}_s$ and $\boldsymbol{n}_l$ are the unit vectors in the directions of the short and long axes, respectively. The total thermophoretic force acting on the ellipsoidal particle is then $\boldsymbol{f}_T = \boldsymbol{f}_s + \boldsymbol{f}_l$, which has a nonzero component perpendicular to the thermal gradient when $\alpha_{T,s} \neq \alpha_{T,l}$, as shown in Fig. 1a.

With eqn (2) and (3), the forces perpendicular and parallel to the thermal gradient are then

$$\boldsymbol{f}_\perp = (\alpha_{T,s} - \alpha_{T,l}) \sin\theta \cos\theta k_B |\nabla T| \boldsymbol{n}_\perp \quad (4)$$

and

$$\boldsymbol{f}_\parallel = -(\alpha_{T,s} \sin^2\theta + \alpha_{T,l} \cos^2\theta) k_B \nabla T, \quad (5)$$

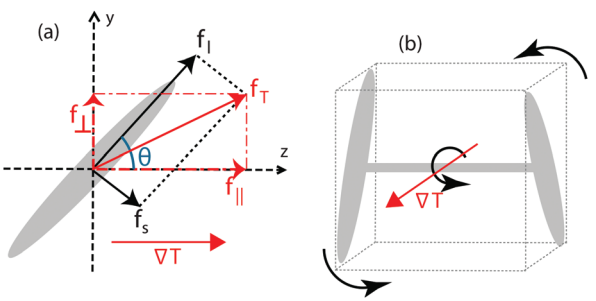

Fig. 1 (a) Diagram of the thermophoretic forces on an anisotropic ellipsoid. (b) Sketch of a minimalistic thermophoretic turbine. Two ellipsoidal blades have opposite orientation angles and their centers are connected by a rigid bond. The rotational direction of the turbine is parallel to the external thermal gradient.

where $\boldsymbol{n}_\perp$ is the unit vector perpendicular to ∇T. For an isotropic particle, $\alpha_{T,s} = \alpha_{T,l}$, such that $\boldsymbol{f}_\perp$ is zero and eqn (5) reduces to eqn (1). How different $\alpha_{T,s}$ and $\alpha_{T,l}$ will depend on the geometry and properties of the object and the solvent. Besides nonsymmetric geometry, heterogeneous material properties may also result in the anisotropy of the thermodiffusion factors. The crucial point now is that a non-zero $\boldsymbol{f}_\perp$ can create a net torque in the direction of the thermal gradient, which allows us to design microscale thermal-gradient-driven turbines. Such turbines do not need macroscopic directional fluid flows as is commonly required for conventional heat engines or turbines.

A minimalistic thermophoretic turbine can be straightforwardly constructed by considering two anisotropic ellipsoids with opposite orientation angles, *i.e.* $\theta' = -\theta$ (the prime refers to the right blade), using a rigid rod to connect the centers of both ellipsoids, as displayed in Fig. 1b. A turbine thus constructed has two-fold rotational symmetry with respect to the temperature gradient, but lacks reflection symmetry. It can be readily shown that the thermophoretic forces on the two blades satisfy the relations, $\boldsymbol{f}'_\parallel = \boldsymbol{f}_\parallel$ and $\boldsymbol{f}'_\perp = -\boldsymbol{f}_\perp$. Therefore, the torque acting on the turbine is parallel to the temperature gradient and reads

$$\mathcal{T} = \boldsymbol{d} \times \boldsymbol{f}_\perp = d(\alpha_{T,l} - \alpha_{T,s}) \sin\theta \cos\theta k_B \nabla T. \quad (6)$$

Here, $\boldsymbol{d}$ is the bond vector connecting the two blades, with $d = |\boldsymbol{d}|$. The direction and magnitude of the torque depend on the difference $\alpha_{T,l} - \alpha_{T,s}$, the externally applied temperature gradient ∇T, and the orientation of the blades, θ. This thermophoretic torque can thus drive the micro-turbine to rotate unidirectionally in an external thermal gradient. The turbine reaches a steady rotational velocity when the hydrodynamic friction balances the thermophoretic torque. The angular velocity is $\omega = \mu_r \mathcal{T}$, with μ_r being the device rotational mobility.

It is instructive to compare the micro-turbine proposed in the present work with the other existing self-thermophoretic rotors.[4,5] Although all these devices rely on thermophoresis, they have significantly different driving mechanisms and potential applications. The present turbine is passively driven by an external thermal gradient whose existence is independent of the turbine. On the other hand, self-thermophoretic rotors are actively driven by a local temperature gradient which is generated by the rotors themselves. Moreover, the turbine exploits the anisotropic thermophoresis, while the self-thermophoretic rotors employ normal isotropic thermophoresis. Consequently, the turbines can recover otherwise wasted heat from existing external thermal gradients, while the self-thermophoretic rotors are not suitable for this purpose.

Simulation method

Computer simulations are performed to test the viability of the proposed thermophoretic micro-turbines. We employ a hybrid scheme of dynamic simulations to account for the drastic differences in both time and length scales between the solvent

molecules and the micro-turbine. The solvent is described by a coarse-grained approach known as multiparticle collision dynamics (MPC),[19–23] while the micro-turbine and its interactions with the solvent are simulated by standard molecular dynamics (MD). In MPC, the solvent is modeled as a large number N of point-like particles of mass m with continuous positions $\boldsymbol{r}_i(t)$ and velocities $\boldsymbol{v}_i(t)$. The algorithm consists of alternating streaming and collision steps. In the streaming step, all the solvent particles move ballistically for a time Δt, $\boldsymbol{r}_i(t + \Delta t) = \boldsymbol{r}_i(t) + \boldsymbol{v}_i(t)\Delta t$. In the collision step, particles are sorted into cubic cells of size a. Then, for each cell, the particle velocities relative to the center-of-mass velocity $\boldsymbol{v}_{cm}$ of the cell are rotated around a random axis $\boldsymbol{n}$ by an angle α, $\boldsymbol{v}_i(t + \Delta t) = \boldsymbol{v}_{cm} + \mathcal{R}(\alpha) \cdot (\boldsymbol{v}_i(t) - \boldsymbol{v}_{cm})$, with $\mathcal{R}(\alpha)$ being the rotation matrix. This coarse-grained collision rule locally conserves mass, linear momentum and kinetic energy. The MPC algorithm has been proved to properly capture hydrodynamic behavior, thermal fluctuations, mass transport, heat conduction and dissipation processes,[19–24] and has been successfully used in the study of colloidal thermophoresis.[14,23,25] In addition, local conservation of the angular momentum in the direction of the temperature gradient (z-axis) is relevant in our simulations. This can be satisfied using the rotational angle in the collision determined according to: $\cos\alpha = (A^2 - B^2)/(A^2 + B^2)$ and $\sin\alpha = 2AB/(A^2 + B^2)$. Here, $A = [\sum \boldsymbol{r}_i \times (\boldsymbol{v}_i - \boldsymbol{v}_i \cdot \boldsymbol{nn})] \cdot \hat{z}$ and $B = [\sum \boldsymbol{r}_i \times (\boldsymbol{n} \times (\boldsymbol{v}_i - \boldsymbol{v}_i \cdot \boldsymbol{nn}))] \cdot \hat{z}$, with $\hat{z}$ being the unit vector of the z direction, and the summation taken over the particles located in the same collision cell.[26] In the simulations we employ standard MPC parameters with the collision time $\Delta t = 0.1$, the average number of solvent particles per cell $\rho = 10$, and the average temperature of the solvent $k_B\bar{T} = 1$. Thus, the dynamic viscosity of the solvent is around $\eta \simeq 3.2$. In the following, all quantities are expressed in terms of the MPC units, where the units of length, mass and energy are separately imposed as a, m and $k_B\bar{T}$, such that the time unit is $a\sqrt{m/k_B\bar{T}}$. The simulation box is a cuboid of dimensions $L_x = L_y = 50$ and $L_z = 34$, with periodic boundary conditions in the x and y directions and a non-slip wall[27] in the z direction. The temperature gradient is applied in the z direction with a boundary thermostat,[23,28,29] ensuring that heat conduction is correctly accounted for.

The efficiency of the previously introduced minimalistic turbine (see Fig. 1b) relies on the thermophoretic anisotropy of each ellipsoid, which is in practice very small. To obtain a reasonably strong anisotropy, we simulate a turbine consisting of two connected triangular blades instead of the ellipsoidal ones, as depicted in Fig. 2a. Each blade is composed of a single layer of monomer beads assembled in the shape of a rigid equilateral triangle. The coupling between the turbine beads and the solvent particles is modeled by potential interactions. Here we consider $U(r) = 4\varepsilon\left[\left(\frac{R}{r}\right)^6 - \left(\frac{R}{r}\right)^3\right] + \varepsilon$ for $r \leq r_c$, with R the bead radii, r the distance from the bead center to the solvent particle, $\varepsilon = 1$ the potential intensity, and $r_c = \sqrt[3]{2}R$ the cutoff radius. This soft repulsive potential has been shown to describe beads with thermophilic behavior and a large thermodiffusion factor.[25] Each blade is composed of 78 beads of radii $R = 1.25$, with neighboring beads separated by $\delta = 1$ (*i.e.* each blade edge has 12 beads and a length $l = 11$). Due to the large bead overlap, the solvent particles (not shown in Fig. 2a) cannot penetrate the blades. Bead–bead interactions only slightly affect the thermophoretic properties of the blade and the local temperature distribution, so that we do not take them into account. In order to avoid the drift of the entire turbine to the warm areas, and to ensure its maximal performance, we fix the center of the turbine in the middle of the simulation box, and allow it to rotate only around the z-axis. The momentum of inertia of the micro-turbine is set as $I = 2 \times 10^5$. The equations of motion are integrated with a velocity-Verlet algorithm[30] with a time step $\delta t = \Delta t/50$. Namely, between two consecutive MPC steps, there are 50 MD steps.

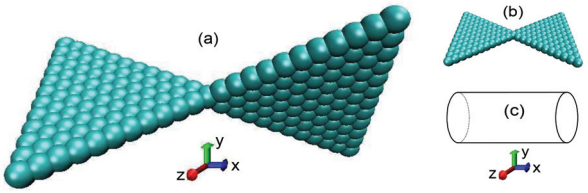

Fig. 2 (a) Simulation model of the external thermal gradient driven micro-turbine. Here, the included angles between the z axis and the left and right blade planes of the turbine are $\theta = -\pi/4$ and $\theta' = \pi/4$, respectively. (b) Symmetric micro-turbine with $\theta = \theta' = -\pi/4$. (c) The cylinder used to approximate the rotational mobility of the micro-turbine.

Results and discussion

Simulation measurements are performed when the system has reached a steady state with a time independent temperature gradient, in which no net solvent flux is present. The angular displacement of the turbine, φ, is averaged over realizations as a function of time and displayed in Fig. 3. Results show that the presence of a temperature gradient induces a unidirectional rotation of the turbine. The turbine motion is subject to thermal fluctuations which can briefly reverse the rotation as shown in the inset of Fig. 3 (also see ESI†); but considering long enough times, the turbine displacement increases linearly with time. As expected by analyzing the torque acting on the turbine in eqn (6), the rotational direction is reversed when the temperature gradient changes sign. In the case of a symmetric turbine where the two blades of the turbine are parallel to each other, *i.e.* $\theta' = \theta$ (as in Fig. 2b), the turbine fluctuates around zero angular position with no net rotation. This clearly indicates that the orientational mismatch between the blades is necessary for the directional rotation of the turbine. The angular velocities ω can be obtained from the slope of the angular displacement curves. Fig. 4 nicely shows how ω increases linearly with ∇T, and varies nonmonotonically with θ. The maximum around $\theta \simeq -\pi/3$ is also consistent with the prediction of eqn (6).

It is enlightening to justify quantitatively the obtained simulation results. Although the simulated turbine is slightly

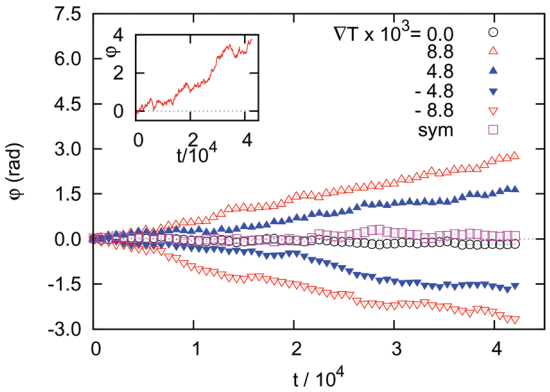

Fig. 3 Averaged angular displacement with time for different applied temperature gradients with $\theta = -\pi/4$. Positive φ corresponds to the counterclockwise rotation of the turbine in Fig. 2a. The notation sym refers to the symmetric micro-turbine, as displayed in Fig. 2b. The inset corresponds to an instantaneous trajectory of the turbine, with the temperature gradient $\nabla T = 0.0088$.

different from the discussed minimalistic analytical version, the calculated expression of the torque in eqn (6) is still valid. When applying eqn (6) to the simulated turbine, θ refers to the included angle between the triangle plane and ∇T. The thermodiffusion factors $\alpha_{T,l}$ and $\alpha_{T,s}$ correspond to the directions parallel and perpendicular to the triangle plane. The distance between the centers of the blades is the bond length $d = 2\sqrt{3}l/3$. To calculate the angular velocity, $\omega = \mu_r \mathcal{T}$, one needs then an estimation of the turbine rotational mobility. To achieve this, we approximate the whole turbine as a cylinder with non-slip surface (Fig. 2c). Considering the size of the beads on the blade edges, the length and diameter of the cylinder are separately taken as $l_H = 2R + \sqrt{3}l$ and $d_H = 2R + l\cos\theta$, which correspond to the turbine dimensions in the x–y and z directions, respectively. The rotational mobility can be expressed as $\mu_r = 3\lambda/\pi\eta l_H{}^3$,[31] with $\lambda = -\ln(d_H/l_H) - 0.662 + 0.917(d_H/l_H) - 0.05(d_H/l_H)^2$. Thus, the rotational velocity becomes

$$\omega = \frac{3\lambda d \sin\theta \cos\theta (\alpha_{T,l} - \alpha_{T,s}) k_B \nabla T}{\pi\eta l_H{}^3}. \quad (7)$$

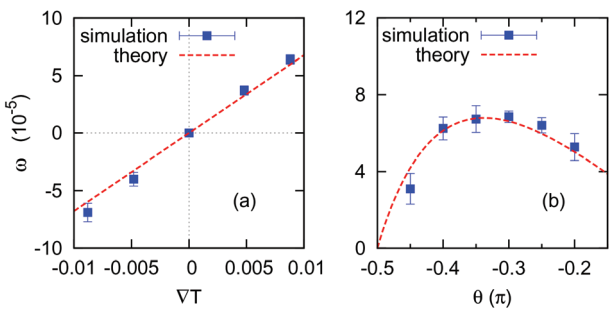

Fig. 4 Angular velocity of the micro-turbine as a function of (a) the temperature gradient and (b) the included angle θ, with the simulation units. Symbols correspond to the simulation results, and lines to the theoretical predictions from eqn (7). In the case of (a), $\theta = -\theta' = -\pi/4$; in the case of (b), the temperature gradient is set as $\nabla T = 0.0088$.

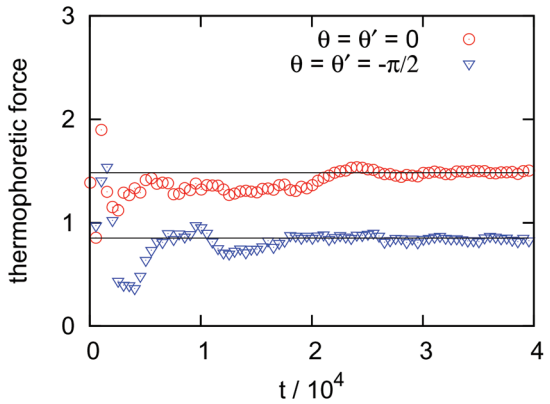

Fig. 5 Thermophoretic forces acting on a fixed triangle blade as a time average, with the temperature gradient $\nabla T = 0.0088$.

Now the thermodiffusion factors $\alpha_{T,l}$ and $\alpha_{T,s}$ of the blades are the only material quantities which still need to be determined. We quantify them by performing independent simulations.[25] Consider a symmetric turbine fixed in space with the blade planes parallel ($\theta = \theta' = 0$) or perpendicular ($\theta = \theta' = -\pi/2$) to the temperature gradient, and then we measure the thermophoretic forces on the blades (see values in Fig. 5). In these configurations only the parallel component of the thermophoretic force, $\boldsymbol{f}_{\parallel}$, is non-vanishing. Quantifying the thermophoretic forces in both cases directly provides us with the calibration of $\alpha_{T,l}$ and $\alpha_{T,s}$ as the ratios between the measured forces and ∇T. The thermodiffusion factors thus measured for the actual device are $\alpha_{T,l} \simeq -168$ and $\alpha_{T,s} \simeq -97$.

With the obtained thermodiffusion factors and eqn (7), the rotational velocity of the micro-turbine can be analytically determined with no adjustable parameters. In Fig. 4a and b, we plot the angular velocity obtained from eqn (7) (dashed lines) and simulation (square symbols) as a function of the temperature gradient and the blade orientation. It is remarkable that this simple analytical approximation can very precisely capture the details of the micro-turbine rotation.

Finally, we discuss the feasibility of experimentally constructing such micro-turbines. Modern micro-fabrication technology can easily produce turbines on the micron scale.[32] The performance of a micro-turbine driven by thermal gradient depends mainly on the thermodiffusion factor α_T and the external temperature gradient ∇T. A rough estimation can be performed by considering a polystyrene particle with 1 μm diameter in water at room temperature typically which has a $\alpha_T \sim 5000$.[33] Under a moderate temperature gradient ($\nabla T \sim 1$ K μm^{-1}) and using eqn (7), we estimate that a polystyrene micro-turbine of ~1 μm can rotate at ~1 round per second.

Conclusions

We have proposed here the principle to design micro-turbines based on the anisotropic thermophoresis effect. The thermophoretic turbines are externally driven by diffusive heat fluxes,

which is a novel concept in comparison to conventional turbines. When coupled with external loads, they can directly harvest mechanical work from the ubiquitous heat flux in microscopic environments, which would otherwise be wasted. At the same time, the extraction of energy facilitates the cooling of heat sources such as micro-processors, which can certainly find advantageous applications. A completely different type of applications can be found in microfluidic devices where thermal gradients can be easily turned on or off locally. This suggests that such micro-turbines can be flexibly utilized to control and drive other micro-devices. Moreover, a well-calibrated turbine can also be employed to detect temperature fluctuations in microscopic settings which are otherwise difficult to measure locally. Various important open questions on the thermophoretic micro-turbine, such as the estimation of its maximum efficiency, warrant further investigation.

Acknowledgements

M.Y. acknowledges the support of the start-up funding from the Institute of Physics, Chinese Academy of Sciences, China. K.C. acknowledges the support from "The Recruitment Program of Global Youth Experts" in China.

Notes and references

1 V. Blickle and C. Bechinger, *Nat. Phys.*, 2012, **8**, 143.
2 F. J. DiSalvo, *Science*, 1999, **285**, 703.
3 L. E. Bell, *Science*, 2008, **321**, 145.
4 H. R. Jiang, N. Yoshinaga and M. Sano, *Phys. Rev. Lett.*, 2010, **105**, 268302.
5 M. Yang and M. Ripoll, *Soft Matter*, 2014, **10**, 1006.
6 C. Ludwig, *Sitzungsber. Preuss. Akad. Wiss., Phys. Math. Kl.*, 1856, **20**, 539.
7 C. Soret, *Arch. Sci. Phys. Nat.*, 1879, **3**, 48.
8 S. Wiegand, *J. Phys.: Condens. Matter*, 2004, **16**, R357.
9 D. Stadelmaier and W. Köhler, *Macromolecules*, 2008, **41**, 6205.
10 J. Giddings, *Science*, 1993, **260**, 1456.
11 S. Duhr and D. Braun, *Proc. Natl. Acad. Sci. U. S. A.*, 2006, **103**, 19678.
12 H.-R. Jiang, H. Wada, N. Yoshinaga and M. Sano, *Phys. Rev. Lett.*, 2009, **102**, 208301.
13 C. J. Wienken, P. Baaske, U. Rothbauer, D. Braun and S. Duhr, *Nat. Commun.*, 2010, **1**, 1093.
14 M. Yang and M. Ripoll, *Phys. Rev. E: Stat. Phys., Plasmas, Fluids, Relat. Interdiscip. Top.*, 2011, **84**, 061401.
15 J. L. Anderson, *Annu. Rev. Fluid Mech.*, 1989, **21**, 61.
16 R. Piazza and A. Parola, *J. Phys.: Condens. Matter*, 2008, **20**, 153102.
17 A. Würger, *Rep. Prog. Phys.*, 2010, **73**, 126601.
18 M. Yang and M. Ripoll, *J. Phys.: Condens. Matter*, 2012, **24**, 195101.
19 A. Malevanets and R. Kapral, *J. Chem. Phys.*, 1999, **110**, 8605.
20 J. T. Padding and A. A. Louis, *Phys. Rev. E: Stat. Phys., Plasmas, Fluids, Relat. Interdiscip. Top.*, 2006, **93**, 031402.
21 R. Kapral, *Adv. Chem. Phys.*, 2008, **140**, 89.
22 G. Gompper, T. Ihle, D. M. Kroll and R. G. Winkler, *Adv. Polym. Sci.*, 2009, **221**, 1.
23 M. Yang and M. Ripoll, *Soft Matter*, 2013, **9**, 4661.
24 M. Ripoll, K. Mussawisade, R. G. Winkler and G. Gompper, *Phys. Rev. E: Stat. Phys., Plasmas, Fluids, Relat. Interdiscip. Top.*, 2005, **72**, 016701.
25 D. Lüsebrink, M. Yang and M. Ripoll, *J. Phys.: Condens. Matter*, 2012, **24**, 284132.
26 M. Yang, M. Ripoll and G. Gompper, *Stochastic rotation dynamics with angular momentum conservation*, 2014, preprint.
27 A. Lamura, G. Gompper, T. Ihle and D. M. Kroll, *Europhys. Lett.*, 2001, **56**, 319.
28 D. Lüsebrink and M. Ripoll, *J. Chem. Phys.*, 2012, **136**, 084106.
29 F. Müller-Plathe, *J. Chem. Phys.*, 1997, **106**, 6082.
30 D. Frenkel and B. Smit, *Understanding Molecular Simulation: From Algorithms to Applications*, Academic Press, San Diego, 2nd edn, 2002.
31 M. M. Tirado, C. L. Martínez and J. G. de la Torre, *J. Chem. Phys.*, 1984, **81**, 2047.
32 Y. L. Zhang, Q. D. Chen, H. Xia and H. B. Sun, *Nano Today*, 2010, **5**, 435.
33 F. M. Weinert and D. Braun, *Phys. Rev. Lett.*, 2008, **101**, 168301.

